Journal of the Korean Geographical Society, Vol.39, No.5, 2004(722~734)

Influence of Tectonic Uplift on Longitudinal Profiles of Bedrock Rivers: Numerical Simulations

Jong Yeon Kim*

융기가 기반암 하상하천의 종단곡선에 미치는 영향에 대한 연구

- 수리 모형을 통한 연구 -

김 종 연*

Abstract : Longitudinal profiles of bedrock rivers play a fundamental role in landscape history by setting the boundary conditions for landform evolution. Longitudinal profiles are changed with climatic conditions, lithology and tectonic movements. Tectonic movement is an important factor controlling longitudinal profiles, especially in tectonically active area where uplift rates are regarded as a major factor controlling channel gradient. However study on bedrock channel has made little progress, because controls over bedrock river incision are yet to be clarified. Previous numerical simulations have used a simple diffusion model, which links together the overall processes of bedrock channel erosion as in other landform evolution models. In this study, previous bedrock incision models based on physical processes (especially abrasion) are reviewed and new modifications are introduced. Using newly formulated numerical model, the role of spatial pattern and intensity of tectonic uplift on changes in river longitudinal profile was simulated and discussed.

Key Words : bedrock rivers, abrasion, numerical simulation, tectonic movements

요약 : 기반암 하상 하천의 종단 곡선은 지형 경관 발달의 기본 조건을 형성 함으로서 경관 변화에 강력한 영향을 행사 한다. 하천 종단 곡선은 기후 환경 조건의 변화, 기반암의 물리 화학적 특성, 지각 운동과 같은 변수들에 의해서 그 형태의 변화를 경험하게 된다. 특히 지각 운동의 시 공간적 양상은 지각 운동이 활발한 혹은 활발했던 것으로 알려진 지역에서 종단곡선에 강력한 영향력을 행사 하는 것으로 추론 되어 왔다. 그러나, 현재까지의 기반암 하상 하천에 대한 연구는 기반암 하상 하천의 침식 작용을 통제 하는 변수들에 대한 이해의 부족으로 답보 상태를 면하지 못하여 왔다. 현대 지형학의 주요 연구 기법인 컴퓨터를 이용한 지형 발달 시뮬레이션은 지형 발달의 단계들을 파악 하는데 유용한 연구 도구로 활용 되어 왔으나, 기반암 하상 하천의 경우 그 이해의 부족으로 인하여 광범위한 응용이 가능한 모형의 마련에 어려움을 겪어 왔다. 그 결과 기존의 연구들은 단순한 확산 모형을 침식의 기본 모형으로 이용 했다. 본 고 에서는 물리적 침식과정에 기반한 기반암 침식 모형들을 검토 수정한 새로운 모형을 소개 하고 해당 모형을 이용하여 지각운동의 시 공간적 분포와 강도가 하천 종단 곡선에 미치는 영향을 시뮬레이션을 통해 모사하고 논의 하였다.

주요어 : 기반암하상하천, 마식, 수리모형, 융기

1. Introduction

The longitudinal profile of the river is a plot of river-bed elevation against distance downstream. Longitudinal profiles are the products of interactions between hydraulic energy and lithologic resistance and so they provide insights into geologic processes and the geomorphic history of an area (Hack, 1973). Hack used a 'steepness index' to describe the form of the channel profile and argued that a high steepness

* Instructor, Department of Geography & Geomatics, University of Glasgow, Scotland, U.K. jkim@geog.gla.ac.uk

index occurs when the channel crosses an area of high erosional resistance ('equilibrium' profile), or is adjusting to a lowered base level (disequilibrium profile). Large rivers with high discharges also have higher values of the index, as the competence of the channel is increased (equilibrium profile). If most of the controlling variables remain relatively constant among a group of channels, then comparison of longitudinal profiles may indicate how the remaining controlling variables influence profile shape (van der Beek and Bishop, 2003). Additionally, because of the low efficiency of erosional processes, the majority of past disturbances are preserved in the long profile.

Longitudinal profiles of bedrock rivers also play a fundamental role in landscape history by setting the boundary conditions for landform evolution. The bedrock channel determines local base level and the lowering rate of bedrock channels controls the rate of erosion and transport processes and forms on the adjacent hillslopes (Seidl *et al.*, 1994). However, erosion rates in bedrock rivers are very low and most erosion processes operate during high magnitude and low frequency floods. Because of this, field process studies are rare except in extreme circumstances and process investigations commonly use analogy from flume studies to provide insight into erosion process in bedrock rivers. However, in many cases flume study results are difficult to apply directly to bedrock rivers, because the appropriate laws to scale from flume to field are unknown. Basin scale studies, including longitudinal profile changes, use the very simple stream power erosion model, which is based on evidence from easily erodible channels.

Tectonic movement is an important factor controlling longitudinal profiles, especially in tectonically active areas where uplift rates are regarded as a major factor controlling channel gradient (Kirby and Whipple, 2001). Previous numerical simulations have used a simple diffusion model, which links together the overall processes of bedrock channel erosion as in other landform evolution models (Whipple and Tucker, 1999). The spatial and temporal patterns of uplift are not necessarily uniform along rivers, but most model approaches assume that rock uplift rate is uniform along the reaches. Studies with shear stress models have shown that spatially variable uplift rates may explain the failure of simple stream power models (Tomkin *et al.*, 2003).

In this study, a new modified incision model is formulated and series of numerical simulation are performed to assess long profile evolution with differential spatial patterns of tectonic movements.

2. Model Formulation

Process-based numerical models of bedrock incision are rare.

Foley (1980) developed the first numerical model that includes the role of sediment particles in the erosion process. His model is a modified version of Bitter's (1963) model that described sand-blast wear on ceramics. Bitter's model was based on the mechanics of individual impacting particles and emphasised that the volume of erosion by impacting particle is governed by the velocity, mass, erosion threshold velocity and hardness of the material.

Sklar and Dietrich (1998) extended Foley's (1980) model to develop a general model for bedrock channel erosion. Their model (Equation 1) can be divided into three principal parts: A: unit erosion by each colliding particle; N: number of sediment particles; and R: relative flux of sediments. The equation is,

$$\varepsilon = \underbrace{\left[\frac{\rho_s \cdot \pi \cdot \sin(\theta) \cdot (u_s^2 + v_s^2) - \varepsilon_t}{\varepsilon_v}\right]}_{A} \cdot \underbrace{\left[\frac{Q_s}{\rho_s \cdot \pi \cdot D^3 \cdot W \cdot \lambda}\right]}_{N} \cdot \underbrace{\left[1 - \frac{Q_s}{Q_t}\right]}_{R}$$

(Equation 1)

where θ is the approach angle of sediment particles (degree), u_s is horizontal velocity of particle (m sec^{-1}), v_s is vertical velocity (m sec^{-1}), Q_s is sediment supply (kg sec^{-1}), Q_t is the transport capacity (kg sec^{-1}), D is sediment size (m), W is channel width (m), ε_v is the energy needed to remove a 'unit volume' of bedrock

from the channel bed (J m^{-3}), and ε_t is the energy threshold which must be exceeded for erosion (J).

Most bedrock channels have sediment supply lower than transport capacity of the flow (*i.e.* $Q_s<Q_t$: Montgomery and Buffington, 1997; Massong and Montgomery, 2000). In these cases, abrasion by sediment is dominant, so as sediment supply increases the erosion rate also increases. However, when sediment supply reaches a limit ($Q_s = Q_t$), sediment particles start to be deposited on the bed and start to play a protective role. As the covered area extends, the erosion rate of the reach declines. Finally, when sediment supply exceeds transport capacity ($Q_s>Q_t$) the bedrock channel becomes an alluvial channel.

Sklar and Dietrich's (1998) model suggested that sediment supply plays a dual role in channel erosion. At low sediment supply ($Q_s/Q_t<0.5$) erosion rates increased quickly with Q_s/Q_t to maximum rates. At $Q_s/Q_t = 0.5$, a further increase in Q_s leads to a decrease in erosion rates. Sklar and Dietrich (1998) described these effects of the role of increasing sediment flux as a transition from a 'tool effects dominates' stage to a 'coverage effects dominates' stage. The relationship between erosion rates and channel slope shows a non-linear pattern with changing slope. It is noteworthy from these results that, for given sediment supply, gentler slopes could result in higher erosion rates than steeper slopes.

To develop an improved model of bedrock erosion, Sklar and Dietrich's (1998) model was tested numerically and modified. In this section, the basic structure and modification procedure are introduced. The basic structure of the modified model is the same as Sklar and Dietrich's model, with the same three terms, representing kinematics, bedload transport rate and relative bedload supply rate (*A*, *N* and *R* terms in Equation 1).

1) Unit Erosion by Sediment Collision

Sklar and Dietrich's model has a dimensional problem in the component representing impact energy by sediment collision, Sklar and Dietrich's (1998) model has dimensions of $ML^{-1}T^{-2}$ and the erosion threshold has dimensions of ML^2T^2, as the units are Joules (1 Joule=1 Newton*meter, 1 Newton=1 kg m sec^{-2}). To solve these problems, the first term has been redefined. The first term of the model is the loss of mass by individual sediment particle impacts (V_e). Sediment particles are regarded as spheres, so the mass of a submerged sediment particle (M_s) of diameter D (m) is, $M_s = \frac{\pi}{6} \cdot (\rho_s - \rho) \cdot D^3$. The particle velocity when it collides with the channel bed (v_i) is given by $v_i = \sqrt{\sin(\theta - S) \cdot (u_s^2 + v_s^2)}$. where θ is approach angle of sediment particle (degree), S is channel slope (degree), u_s is horizontal velocity of the particle and v_s is it's vertical velocity.

The approach angle and horizontal and vertical velocity are controlled by the physical characteristics of saltation, which is governed by shear stress and particle size. The impact force increases when the angle of impact and particle velocity increases (Hussainova, 1999). When particles collide with the channel bed, the impact angle depends on channel slope. This means that in a steeper channel the impact angle is reduced by the effect of channel slope. This means in turn that reaches with locally reverse slopes should show higher erosion rates than other parts of the bed.

Combining equations 2 and 3, the energy (F_i, J) produced by a sediment impact is

$$F_i = \frac{\pi}{12} \cdot (\rho_s - \rho) \cdot D^3 \cdot \sin(\theta - S) \cdot (u_s^2 + v_s^2) \quad \text{(Equation 2)}$$

Erosion occurs when the impact energy exceeds the threshold for erosion (ε_t), which is determined by lithology and other geologic variables. The volume of channel bed removed by an impacting particle can be estimated by dividing the impact energy by the energy to be needed to remove a 'unit' volume of bedrock from channel bed (ε_v, J m^{-3}), hence

$$V_e = \frac{F_i - \varepsilon_t}{\varepsilon_v} = \frac{\frac{1}{12} \cdot (\rho_s - \rho) \cdot D^3 \cdot \pi \cdot \sin(\theta - S) \cdot (u_s^2 + v_s^2) - \varepsilon_t}{\varepsilon_v} \quad \text{(Equation 3)}$$

In Equation 3, the volume removed from the channel bed increases with sediment diameter (D), approach angle (θ), sediment density, and horizontal and vertical velocity of particles. The characterization of lithologic resistance is discussed below.

2) Sediment Dynamics

Saltation is one of the processes of bedload transport and is an intermediate mode of transport between rolling and suspension (Gilbert, 1914; Francis, 1973). The physical characteristics of saltation, including the horizontal particle velocity, approach angle and saltation length, are critical factors in determining erosion rate by sediment collision in bedrock rivers (Foley, 1980; Sklar and Dietrich, 2004). There is no sharp division between bed load transport and suspended load transport in natural conditions. However, several suspension thresholds have been identified. The initial bedload transport occurs at transport stage (dimensionless shear stress/ dimensionless critical shear stress: τ^*/τ^*cr) approaching 1.5 and saltation dominates from 2.9. Dimensionless shear stress (τ^*) and shear velocity (u^*) are the major variables used to describe and to estimate the sediment particle movements (Murphy and Hooshiari, 1982). However, most experiments have used fine or low-density particles with low discharges, creating a scaling problem in applying the results to gravel and bedrock channel beds. To find a suitable model of gravel saltation to use here in the incision model, eight previous models are compared numerically. The vertical velocity of transporting particles (v_s) is taken as the particle's fall velocity (w) (Julien, 1995), given by ω = 3.8203*exp(1.1627 · $LogD$).

The approach angle (θ) is an important variable determining the kinematics of collision. Erosion rates increase as the impact angle (θ-S) increases (Shimizu *et al.*, 1999). The approach angle was estimated using data from Wiberg and Smith's (1985) graph which is based on data from previous studies, yielding the equation

$$\theta = 0.42 - \left(0.002 \cdot \frac{\tau^*}{\tau^*_{cr}}\right) \qquad \text{(Equation 4)}$$

Thus, the equations used in this model for horizontal particle velocity and saltation length (λ) are (Nino *et al.*, 1994);

$$\frac{u_s}{u^*_{cr}} = -1.4445 + \left[2.4099 \cdot \left(\frac{\tau^*}{\tau^*_{cr}}\right)\right] \qquad \text{(Equation 5)}$$

$$\frac{\lambda}{D} = -3.826 + 7.6322 \cdot \left(\frac{\tau^*}{\tau^*_{cr}}\right) \qquad \text{(Equation 6)}$$

The major variables that affect the resistance to erosion are rock mass strength, which is determined by the character of the rock forming minerals, weathering, and the density and spacing of joints and fissures in the rock mass (Day, 1980).

3) Lithologic Characterization

Lithology of the channel is a critical factor affecting erosion rates, as it influences resistance to erosion, as in the ε_t and ε_v terms of Equation 3. Most geomorphic studies of bedrock resistance have used Schmidt hammers in the field to characterize lithology (Selby, 1980; Wohl and Ikeda, 1998; Snyder *et al.*, 2003). Although it is simple to use in the field, there is no clear physical explanation of the relation between the Schmidt hammer readings and erosion rates. As a result, Schmidt hammer readings prove to be poor predictors of erosion (Wohl and Ikeda, 1998). Foley (1980) used the elastic index, which is widely used in engineering studies of wear, to define lithologic properties in his model. Two different lithologic constraints are used in Foley's model. The first is the energy needed to remove a 'unit' volume of bedrock from the channel bed (ε_v). Bitter (1963) and Foley (1980) formulated ε_v (J m^{-3}) as,

$$\varepsilon_v = c_l \cdot \frac{z^2}{E} \qquad \text{(Equation 7)}$$

where c_l is an empirical constant (19.21 adopted by Foley), z is the elastic load limit (N m^{-2}), and E is the Young's modulus (N m^{-2}). The elastic load limit is determined by a uniaxial compression test and Young modulus is determined by a bending test.

The second lithologic constraint is the threshold energy of erosion (ε_t and K). Foley (1980) used a 'speed' term (m sec^{-1}) as a threshold for erosion. If sediment particle velocities are slower than the erosion threshold, there should be no erosion. Sklar and Dietrich (1998) changed this to a kinematic (energy) term. This term is difficult to quantify in either formulation. The modification used here is based on Sklar and Dietrich's model, but Foley's characterization is used rather than tensile strength.

4) Number of Sediment Particles

The second term of the model is the number of particle impacts for unit channel width and length, in effect the bedload transport rate (the 'N' term in Equation 1). As in the kinematic part of the model (the term 'A' in equation 1), sediment particles are regarded as spheres.

As there is a protective role of sediment cover, a necessary condition for bedrock incision is that the supply of sediment to the reach does not cover the channel bed (Hancock *et al.*, 1998). To model channel bed erosion reliably, the bedload transport capacity of the flow (q_t) should be considered properly. Transport capacity is a function of channel shear stress and critical shear stress and sediment size. The Mayer-Peter and Muller-type bedload equation (q_t) is used here, given by

$$q_t = 8 \cdot \left(\frac{(\rho_s - \rho) \cdot g \cdot D^3}{\rho_s} \right)^{0.5} \cdot (\tau^* - \tau^*_{cr})^{1.5} \quad \text{(Equation 8).}$$

As sediment flux increases, the number of impacts (N_i) is also increased. N_i is given by

$$N_i = \left[\frac{q_s}{\frac{1}{6} \cdot \rho_s \cdot \pi \cdot D^3 \cdot \lambda} \right] \quad \text{(Equation 9).}$$

It can be assumed that a constricted channel has higher erosion than a wider reach, as sediment flux per unit width is increased by constriction.

5) Effective and Relative Sediment Flux

As the transport stage increases, the number of particles that are transported by saltation is decreased. Abbot and Francis's (1977) data were analysed to scale the number of particles by increasing transport stage (τ^*/τ^*_{cr}). Regression analysis of their data gives the proportion of particles moving through saltation as,

$$q_{se} = q_s \cdot \left[1 - \left(0.0088 + 0.26 \cdot \ln\left(\frac{\tau^*}{\tau^*_{cr}} \right) \right) \right] (R^2 = 0.98)$$

(Equation 10)

Where, q_{se} is effective sediment flux (kg/sec).

Relative sediment flux (Q_s/Q_t) is the relative sediment flux entering a reach. If this flux exceeds 1.0 the reach will be covered by sediment particles so protecting the bed. The effective discharge and sediment supply for annual erosion rates are scaled as 2% of annual flow time.

The threshold of erosion initiation (ε_t) is set as 0, as the initial point of erosion is not clear in quantitative terms and has little effect on calculated incision rates. By synthesizing the three parts above, the revised incision model is as follows

$$\varepsilon = K_1 \cdot K_2 \cdot \frac{\sin(0.42 - 0.002 \cdot \tau^*/\tau^*_{cr}) \cdot ((u^*_{cr})^2 \cdot (-1.44 + 2.41 \cdot \tau^*/\tau^*_{cr})^2 + K_3}{-3.83 + 7.63 \cdot \tau^*/\tau^*_{cr}}$$

(Equation 11)

Where K_1 is geologic constant ($K_1 = \frac{1}{2 \cdot \varepsilon_v}$), K_2 sediment supply constant ($K_2 = q_{se} \cdot \frac{Q_s}{Q_t}$ with $q_{se} \cdot \frac{Q_{se}}{W}$) and K_3 is threshold constant for initiation of erosion ($K_3 = \omega^2 - 6 \cdot v_{cr}^2$).

3. Simulation Results and Discussion

Uplift of the entire reach was simulated initially. The conditions of each experiment are set to check the effect of uplift along the reach. Uplift varies linearly from the top to the bottom of the reach (Table 1).

The modelling is based on the characteristics of the River Etive, a bedrock river in the Scottish high-

Table 1. Uplift settings of experiments T1, T2, T3 and S3.

	Experiment T1	Experiment T2	Experiment T3	Experiment S3
Uplift rates at the upstream end of reach	1 mm/year	0 mm/year	3 mm/year	0 mm/year
Uplift rates at the downstream end of reach	0 mm/year	1 mm/year	0 mm/year	0 mm/year
Temporal pattern	Continuous	Continuous	Continuous	None

lands exhibiting knickpoints (Kim, 2004). Drainage basin area was measured on the Ordnance Survey 1:25,000 Pathfinder series. Drainage area was found to increase linearly with distance downstream (Drainage Area =15+(6.27*distance), R^2=0.97). The discharge per unit area (m^3/m^2) is based on nearest SEPA(Scottish Environmental Protection Agency) station at Bridge of Orchy (record from 1977 to 2001) also has positive linear relationship with distance (Q = 4.1+(1.04**distance*), (R^2=0.94)).

Experimental conditions include downstream fining with initial particle size of 40mm. Sediment concentration ratio (Q_s/Q) was constant (0.1333). Discharge and sediment flux both increased systematically downstream. The sediment flux in this simulation is the effective sediment flux, which depends on the transport stage. Initial channel gradient is fixed at 0.01 and is taken from a typical bedrock reach in the River Etive.

1) Decreasing Uplift Downstream: Experiment T1

Uplift rate in this experiment is 1 mm per year at the top of the reach decreasing downstream to 0 mm. Discharge and sediment supply increase downstream as in previous experiments. Particle size decreases exponentially downstream (α=-0.0002) from 40mm at the upstream boundary. Bed height, channel gradient and erosion rates are recorded every 2,000 years through the experiment. If there were no erosion along the channel, the gradient after 10 ka would be 0.011 (a 10% increase in channel gradient).

The change of profile form through time suggests that the channel can be divided into two sub-reaches. The upper reach shows a net increase in height (final height > initial height) with the greatest increase at the top of the reach decreasing toward an equilibrium point (initial height=final height). However, this does not imply that the erosion rates

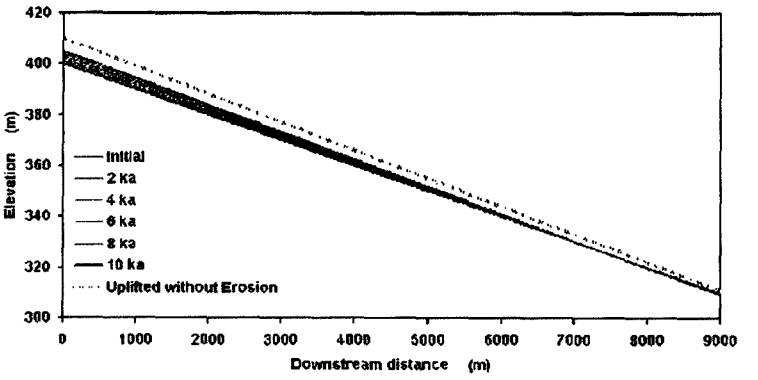

Figure 1. Longitudinal profile of Experiment T1

Elevation at the upstream section of the reach rises through time, due to uplift. The downstream section of the reach experiences lowering, as uplift rate is low and erosion is active.

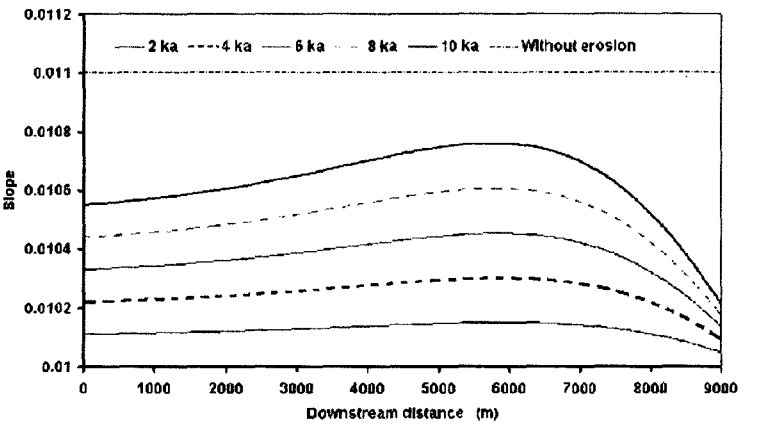

Figure 2. Changes in bed slopes in Experiment T1

If there were no erosion at all, resulting slope would reach 0.11 for whole reach. Slope increases through time due to rapid uplift at the upstream section. Slope slightly steepens downstream to some part and declines further downstream. There is a declining rate of downstream reach slope decline through time.

increase along the whole reach, as the uplift rate is maximized at the top of the channel. The channel gradients increase through time as a result of unequal uplift along the channel. The overall spatial pattern of the channel gradient along the channel is similar to the case without uplift. As sediment size decreases downstream, erosion along the channel also changes due to the changes in effective sediment flux and transport stage. Overall slope is steepened through time by the rapid uplift in the upstream reach.

The ratio of bed slope in experiment T1 and the equivalent non-uplift case increases from 1.001 (2 ka) to 1.005 at 10 ka. The ratio has maximum values in the upstream reach and decreases downstream. It shows only very slight changes in channel gradients due to uplift. Uplift alone causes channel gradient to steepen by 1% every 1000 years, if there is no erosion. These results suggest that the erosive force in bedrock channel equilibrates with uplift quickly, as a consequence of increasing channel gradient. As uplift rate is highest upstream, the bed elevation change rate becomes negative in the upstream part of the reach. That is, erosive forces overcome uplift 7.5 km along the reach and the channel incises. Rapid uplift upstream causes the steepening of the reach, and this steepening of the reach is accelerated the erosion by increased transport stage. Erosion rates are maximised at the top of the channel and decrease downstream. The intensity of erosion in the upstream reach increased to > 3.5 times erosion in the stable case (S3). In the stable conditions, maximum erosion rates along the channel were less than 0.14 mm/year. The erosion rates along the river are strongly controlled by the uplift rates and the spatial pattern of uplift rather than other factors.

The equilibrium point (initial height = final height, so elevation change is 0) moves upstream through time at a decreasing rate (from 25mm per year initially to 20mm per year after 10 ka). The speed of the upstream migration is higher than vertical erosion rates that also get slower as the equilibrium point moves upstream. The migration speed depends on the erosional force at the equilibrium point.

Experiment T3 has the same settings except uplift rates. The longitudinal profile at 10 ka shows similar pattern to experiment T1 (Figure 3). Increased uplift rate raises the elevation further than in the low uplift setting. The equilibrium point, where the elevations before and after uplift are the same, is formed fur-

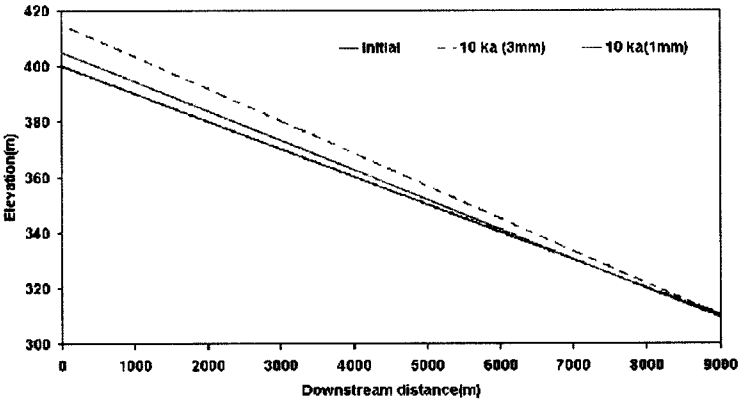

Figure 3. Longitudinal profiles of Experiment T1 and Experiment T3.

Rapid uplift produced the steeper slope along the reach. The red line is the profile of 3mm/year uplift and blue line is that of 1mm/year uplift.

ther downstream.

When the upstream uplift rate is increased to 3mm per year, the erosion rates increase more than the uplift rate (Figure 4). The relative erosion, calculated by dividing the erosion rates in the 3mm uplift case by those in the 1mm uplift case, exceeds 3 along the reach. This ratio increases downstream and decreases through time. Considering the bed elevation changes due to the contributed effect of uplift and erosion, the difference of slope between 3mm uplift and 1mm uplift cases becomes progressively greater. This result suggests that the uplift rate is the most influential factor changing the form of longitudinal profiles in tectonically active areas.

2) Increasing Uplift Downstream: Experiment T2

The uplift rate in this experiment was 0 mm per year at the top of reach, increasing downstream to 1 mm per year at the downstream end of the reach. This is the inverse uplift pattern to Experiment T1, but the mean uplift rate for the whole reach is the same in both cases. All conditions- discharge, sediment supply and grain size- are the same as in experiment T1. The longitudinal profile produced by downstream increase in tectonic uplift can also be

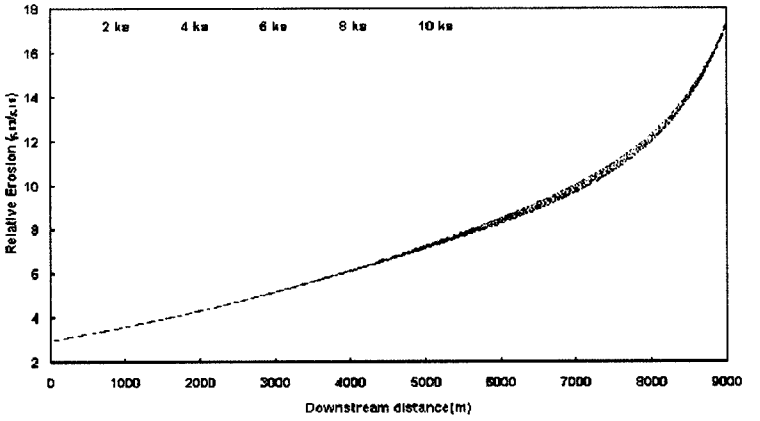

Figure 4. Relative erosion in the 3mm uplift case (Experiment T3) compared to the 1mm uplift case (Experiment T1)

Relative erosion rate is calculated by dividing net erosion rate of T3 by T1. The relative erosion rate increases downstream.

divided into two parts (Figure 5).

The uppermost 110m section of the channel is eroded slightly (initial elevation is greater than the 10 ka elevation), whereas the rest of the reach shows a net increase in elevation. This means that erosion in most of the reach is insufficient to overcome uplift. Increasing transport stage and decreasing particle size results in decreasing slope downstream, but the spatial pattern of erosion is not as clearly related to slope as in experiment T1. Erosion rates increase downstream, but the pattern of increase is strongly influenced by the uplift rate.

Numerical simulation with various spatial patterns of erosion suggests that changes of longitudinal profile are controlled by uplift rate and erosion in the specific reach. The main control over erosion along the channel is the transport stage, which affects the physical aspects of saltation, impact kinematics and the number of impacting particles. Bed elevation changes for 10ka, based on height change from the initial longitudinal profile show that transport stage has a weak relationship with bed elevation change (Figure 6). As a result of tectonic movement Experiment T1 has the highest transport stage

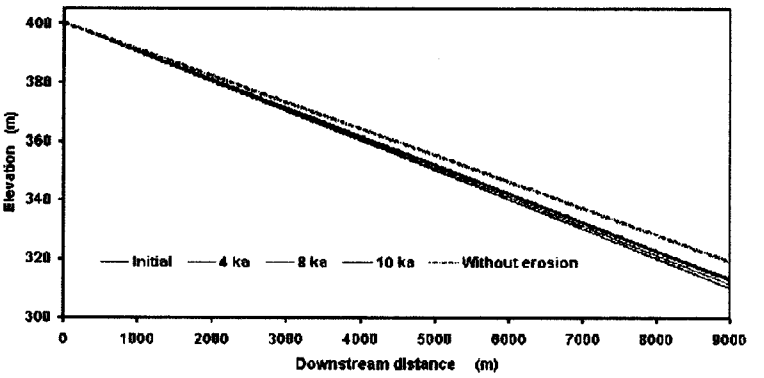

Figure 5. Longitudinal profiles of Experiment T2

Like Experiment T1, most of the reach increases in elevation due to uplift, except at the upstream end of the reach where uplift rate is zero.

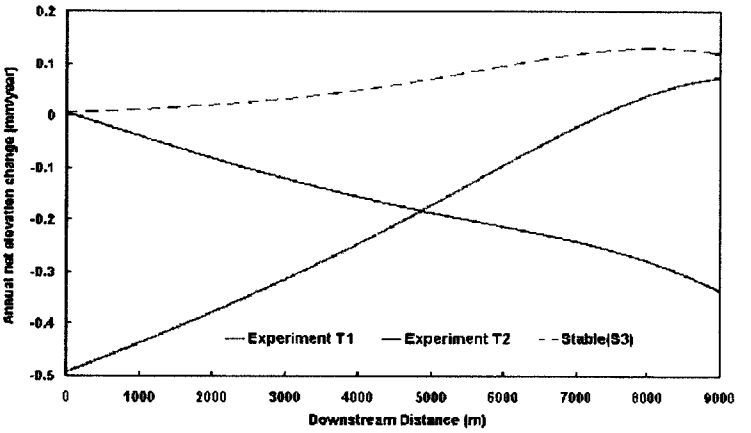

Figure 6. Annual elevation changes calculated from the change from initial heights (initial elevation-final elevation)

Negative values of elevation change in this figure mean increasing elevation. Simple elevation changes of T1 (decreasing uplift rate downstream), T2 (increasing uplift rate downstream) and S3 show that the tectonic uplift rate controls elevation changes. However, this figure does not show the erosion pattern of each case.

and overall erosion rate, due to the steepening of the reach.

However, when tectonic uplift is deducted from elevation changes (net erosion rate), the spatial pattern of net erosion rate shows a different pattern from elevation changes (Whipple, 2001). The spatial pattern of net erosion in the stable case (S3) and the uplifting case of experiment T2 can be explained by the slope changes, but the experiment T2 has gentler slope than stable case (Figure 7). So it is suggested that all erosion rates have a strong relationship with the uplift pattern and intensity rather than with hydraulic variables. This simulation result supports the argument that sediment flux and uplift rate are major controlling factors in uplifted areas (Humphrey and Konrad, 2000).

As expected, different uplift patterns produce different erosion patterns along the channel and different channel gradients for the relatively short term (10 ka). It is also noteworthy that the increase in uplift rates in lower reaches causes a strong increase in erosion.

Theoretical arguments suggested that the increase in uplift rates lead to the higher erosion rates that lead to steady state. The steady-state profile is the general term to interpret the long profile formed by the balance between the rate of incision and rate of uplift (Burbank *et al.*, 1996; Pazzaglia and Brandon, 2001). Net erosion rate changes along the reach in Figure 7 show similar spatial patterns to uplift rates, but the erosion rate of the point where uplift is most rapid is just half of the maximum uplift rate. Meanwhile, the erosion rate at the point where the uplift rate is minimum (0) is higher than the uplift rate. An 'equilibrium' between uplift rate and erosion rate is formed and is extended into the zone of net erosion, but the speed of extension is slow while uplift persists. So, if uplift ceased and hydraulic conditions were sustained, the dominance of erosion would be extended to the whole reach. The speed of extension depends on uplift rate, hydraulic variables and lithology (Koons, 1989; Kooi and Beaumont, 1994).

It is also noteworthy that net erosion rates in the downstream reach in Figure 7 are not coinciding with the uplift pattern. This longitudinal pattern of net erosion results from the erosion rate by abrasion, which is controlled by transport stage. Downstream fining of sediment grains and effective sediment flux are responsible for this changing pattern. When the

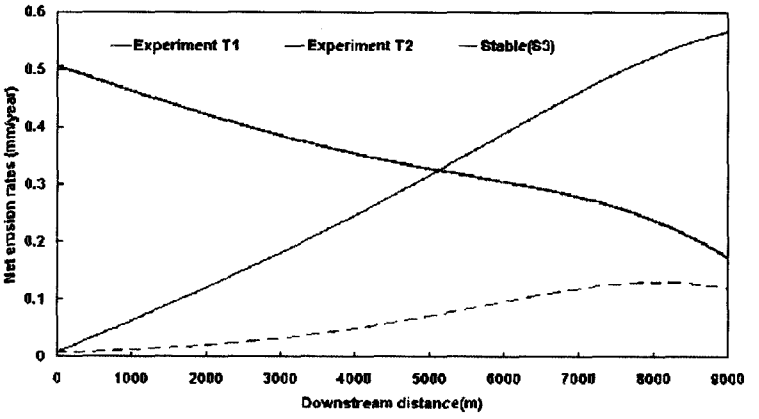

Figure 7. Annual erosion rates with consideration of uplift

The elevation changes by the uplift are deduced from total elevation changes. So this figure shows the net erosion rate due to the erosion process. Erosion rates of T1 (decreasing uplift rate downstream), T2 (increasing uplift rate downstream) and S3 show erosion rate patterns similar to the uplift rates and uplift triggers severe erosion along the reach.

downstream end of the reach was uplifted, a knickpoint is formed, but the pattern of change of the knickpoint was lying back with very slow retreat. From field studies in tectonically active areas, knickpoints formed by base level change retreat upstream with higher erosion rates downstream of the knickpoint (*i.e.* Righter, 1997; Pazzaglia and Brandon, 2001).

4. Conclusion

A new modified model of bedrock channel incision with abrasion is introduced in this study.

The basic structures of the improved and modified model of bedrock abrasion has three separate terms representing: (i) unit erosion by individual impact kinematics of the sediment particles; (ii) number of sediment particles as a function of bedload transport rate and transport mode; and (iii) relative bedload supply rate. The modifications involved calibration of the impact force as a function of sediment particle size, changes in saltation characteristics, and the introduction of an effective sediment flux term (Qse). The sensitivity tests of sediment dynamics suggested that the flume study results with relatively large particles (Nino *et al.*, 1994) properly represent the sediment dynamics for this study.

It was found that the spatial pattern of tectonic movement is the most influential factor for the erosion rate change along the river. Even though the mean uplift rate for the whole river reach is the same, different spatial uplift rates produced different longitudinal profiles as a result of interactions with erosion rate. It is suggested that the erosion rate in an uplifting area is controlled by the influence of uplift rate on slope. This simulation result supports the idea of steady-state erosion that the increase in uplift rates leads the higher erosion rates to achieve the steady state. An 'equilibrium' between uplift rate and erosion rate is formed in the middle of the reach and would extend to the whole reach. The speed of extension depends on uplift rate, hydraulic variables and lithology.

It should be noted that additional physical modelling and field test should be followed to justify newly introduced model.

Acknowledgements

This paper is the part of the Ph.D dissertation of the author. Author would like to thanks to Professors Trevor Hoey, Professor Paul Bishop (Centre for Geosciences, University of Glasgow) and Dr. Niels Hovius(University of Cambridge) for their comments and discussion. Department of Geography & Geomatics, University of Glasgow provided financial support for author's research activities.

References

Abbott, J.E. and Francis, J.R.D.,1977, Saltation and suspension trajectories of solid grains in a water stream, *Philosophical transactions of the Royal Society of London*, 284(A), 225-254.

van der Beek, P. and Bishop, P., 2003, Cenozoic river profile development in the Upper Lachlan catchment (SE Australia) as a test of quantitative fluvial incision models, *Journal of Geophysical Research*, 108(B), doi:10.1029/2002JB002125.

Bitter, J.G.A., 1963, A study of erosion phenomena: Part 1, *Wear*, 6, 5-21.

Burbank, D.W., Leland, J., Fielding, E., Anderson, R.S., Brozovic, N., Reid, M.R., and Duncan, C., 1996, Bedrock incision, rock uplift, and threshold hillslopes in the northwestern Himalaya, *Nature*, 379, 505-510.

Day, M.J., 1980, Rock hardness: field assessment and geomorphic importance, *Professional*

Geographer, 32, 72-81.

Foley, M.G., 1980, Bedrock incision by streams, *Geological Society of America Bulletin*, 91 (part 2), 2189-2213.

Francis, J.R.D., 1973, Experiments on the motion of solitary grains along the bed of a water-stream, *Philosophical transactions of the Royal Society of London*, 332(A), 443-471.

Gilbert, G.K., 1914, *The transportation of debris by running water*, U.S. Geological Survey, Professional Paper, 86.

Hack, J.T., 1973, Stream profile analysis and stream-gradient index, *Journal of Research, U.S. Geological Survey*, 1, 421-429.

Hancock, G.S., Anderson, R.S., and Whipple, K.X., 1998, *Beyond power: bedrock river incision process and form*, in Tinkler, K.J. and Wohl, E.E. (Eds.), *Rivers over Rock: Fluvial Processes in Bedrock Channels*, American Geophysical Union, Washington.

Humphrey, N.F. and Konrad, S.K., 2000, River incision or diversion in response to bedrock uplift, *Geology*, 28, 43-46.

Hussainova, I.K.I, 1999, Investigation of particle-wall impact process, *Wear*, 233-235, 168-173.

Jullien, P.Y., 1995, *Erosion and Sedimentation*, Cambridge University Press, Cambridge.

Kirby, E. and Whipple, K.X., 2001, Quantifying differential rock-uplift rates via stream profile analysis, *Geology*, 29, 415-418.

Kooi, H. and Beaumont, C., 1994, Escarpment evolution on high-elevation rifted margins: Insights derived from a surface processes model that combines diffusion, advection, and reaction, *Journal of Geophysical Research*, 99(B), 12191-12209.

Koons, P.O., 1989, The topographic evolution of collisional mountain belts: a numerical look at the Southern Alps, New Zealand, *American Journal of Science*, 289, 1041-1069.

Massong, T.M. and Montgomery, D.R., 2000, Influence of sediment supply, lithology, and wood debris on the distribution of bedrock and alluvial channels, *Geological Society of America Bulletin*, 112, 591-599.

Montgomery, D.R. and Buffington, J.M., 1997, Channel-reach morphology in mountain drainage basins, *Geological Society of America Bulletin*, 109, 596-611.

Murphy, P.J. and Hooshiari, H., 1982, Saltation in water dynamics, *Journal of Hydraulic Engineering*, 108, 1251-1267.

Nino, Y., Garcia, M. and Ayala, L., 1994, Gravel saltation: experiment, *Water Resources Research*, 30, 1907-1914.

Pazzaglia, F. J. and Brandon, M.T., 2001, A fluvial record of longterm steady-state uplift and erosion across the Cascadia forearc high, Western Washington state, *American Journal of Science*, 301, 385-431.

Righter, K., 1997, High bedrock incision rates in the Atenguillo river valley, Jarisco, Western Mexico, *Earth Surface Processes and Landforms*, 22, 337-343.

Seidl, M.A., Dietrich, W.E. and Kirchner, J.W., 1994, Longitudinal profile development into bedrock: an analysis of Hawaiian channels, *Journal of Geology*, 102, 457-474.

Selby, M. J., 1980, A rock mass strength classification for geomorphic purposes: with tests from Antartica and New Zealand, *Zeitschrift fur Geomorphologie*, 24, 31-51

Shimizu, K., Noguchi, T., Seitoh, H., and Muranaka, E., 1999, FEM analysis of the dependency on impact angle during erosive wear, *Wear*, 233-235, 157-159.

Sklar, L.S. and Dietrich, W.E., 1998, River longitudinal profiles and bedrock incision models: streampower and the influence of sediment supply, in Tinkler, K.J. and Wohl, E.E. (eds.), *Rivers over Rock: Fluvial Processes in Bedrock Channels*, American Geophysical Union, Washington.

Sklar, L.S. and Dietrich, W.E., 2004, A mechanistic

model for river incision into bedrock by saltating bed load, *Water Resources Research*, 40, doi:10.1029/2003WR002496.

Snyder, N.P., Whipple, K.X., Tucker, G.E. and Merritts, D.J., 2003, Channel response to tectonic forcing: field analysis of stream morphology and hydrology in the Mendocino triple junction region, northern California, *Geomorphology*, 53, 97-127.

Tomkin, J.H., Brandon, M.T., Panzzaglia, F.J., Barbour, J.R. and Willett, S.D., 2003, Quantitative testing of bedrock incision models for the Clearwater River, NW Washington State, *Journal of Geophysical Research*, 108(B), doi:10.1029/2001JB000862.

Whipple, K.X. and Tucker, G.E., 1999, Dynamics of the stream-power river incision model: implication for the height limits of mountain ranges, landscape response time scales, and research needs, *Journal of Geophysical Research*, 104(B), 17661-17674.

Whipple, K.X., 2001, Fluvial landscape response time: how plausible is steady-state denudation, *American Journal of Science*, 301, 313-325.

Wiberg, P.L and Smith, J.D., 1985, A theoretical model for saltating grains in water, *Journal of Geophysical Research*, 90(C), 7341-7354.

Wohl, E.E. and Ikeda, H., 1998, Patterns of bedrock channel erosion on the Boso Peninsula, Japan, *Journal of Geology*, 106, 331-345.

Received August 20, 2004
Accepted December 8, 2004

Correspondence : Jong Yeon Kim, Dept. of Geography & Geomatics, University of Glasgow, Scotland, U.K.(jkim@geog.gla.ac.uk, phone: 44-141-330-4445, fax: 02-882-9873)

교 신 : 김 종 연 , Dept. of Geography & Geomatics, University of Glasgow, Glasgow, G12 8QQ, Scotland, United Kingdom(이메일 : jkim@geog.gla.ac.uk 전화: 44-141-330-4445 팩스 : 02-882-9873)